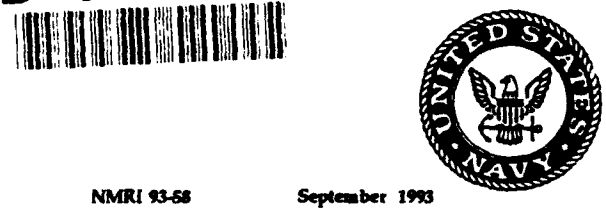

Naval Medical Research Institute

Bethesda, MD 20889-5607 NMRI 93-58 September 1993

ELASTANCE AND INERTANCE IN UBA BREATHING BAG SIMULATION AND DESIGN

D. D. Joye
N. A. Carlson
J. R. Clarke

Naval Medical Research
and Development Command
Bethesda, Maryland 20889-5606

Department of the Navy
Naval Medical Command
Washington, DC 20372-5210

NOTICES

The opinions and assertions contained herein are the private ones of the writer and are not to be construed as official or reflecting the views of the naval service at large.

When U. S. Government drawings, specifications, or other data are used for any purpose other than a definitely related Government procurement operation, the Government thereby incurs no responsibility nor any obligation whatsoever, and the fact that the Government may have formulated, furnished or in any way supplied the said drawings, specifications, or other data is not to be regarded by implication or otherwise, as in any manner licensing the holder or any other person or corporation, or conveying any rights or permission to manufacture, use, or sell any patented invention that may in any way be related thereto.

Please do not request copies of this report from the Naval Medical Research Institute. Additional copies may be purchased from:

National Technical Information Service
5285 Port Royal Road
Springfield, Virginia 22161

Federal Government agencies and their contractors registered with the Defense Technical Information Center should direct requests for copies of this report to:

Defense Technical Information Center
Cameron Station
Alexandria, Virginia 22304-6145

TECHNICAL REVIEW AND APPROVAL

NMRI 93-58

The experiments reported herein were conducted according to the principles set forth in the current edition of the "Guide for the Care and Use of Laboratory Animals," Institute of Laboratory Animal Resources, National Research Council.

This technical report has been reviewed by the NMRI scientific and public affairs staff and is approved for publication. It is releasable to the National Technical Information Service where it will be available to the general public, including foreign nations.

ROBERT G. WALTER
CAPT, DC, USN
Commanding Officer
Naval Medical Research Institute

UNCLASSIFIED

SECURITY CLASSIFICATION OF THIS PAGE

REPORT DOCUMENTATION PAGE

1a. REPORT SECURITY CLASSIFICATION UNCLASSIFIED	1b. RESTRICTIVE MARKINGS
2a. SECURITY CLASSIFICATION AUTHORITY	3. DISTRIBUTION/AVAILABILITY OF REPORT Approved for Public Release; distribution is unlimited.
2b. DECLASSIFICATION/DOWNGRADING SCHEDULE	
4. PERFORMING ORGANIZATION REPORT NUMBER(S) NMRI 93-58	5. MONITORING ORGANIZATION REPORT NUMBER(S)
6a. NAME OF PERFORMING ORGANIZATION Naval Medical Research Inst. — 6b. OFFICE SYMBOL (If applicable)	7a. NAME OF MONITORING ORGANIZATION Bureau of Medicine and Surgery
6c. ADDRESS (City, State, and ZIP Code) 8901 Wisconsin Avenue Bethesda, Maryland 20889-5607	7b. ADDRESS (City, State, and ZIP Code) Department of the Navy Washington, DC 20372-5120
8a. NAME OF FUNDING/SPONSORING Naval Medical Research and Development Command — 8b. OFFICE SYMBOL (If applicable)	9. PROCUREMENT INSTRUMENT IDENTIFICATION NUMBER
8c. ADDRESS (City, State, and ZIP Code) 8901 Wisconsin Avenue Bethesda, Maryland 20889-5605	10. SOURCE OF FUNDING NUMBERS PROGRAM ELEMENT NO. 63713N — PROJECT NO. M0099.01B — TASK NO. 1005 — WORK UNIT ACCESSION NO. DN477506

11. TITLE (Include Security Classification)

ELASTANCE AND INERTANCE IN UBA BREATHING BAG SIMUATION AND DESIGN

12. PERSONAL AUTHOR(S)
JOYE, D.D., N.A. CARLSON, AND J.R. CLARKE

13a. TYPE OF REPORT	13b. TIME COVERED	14. DATE OF REPORT (Year, Month, Day)	15. PAGE COUNT
TECHNICAL REPORT	FROM 6/90 TO 8/92	SEPTEMBER 1993	

16. SUPPLEMENTARY NOTATION **Dr. Joye at: Department of Chemical Engineering; Villanova University; Villanova, PA 19085 Dr. Clarke at: Navy Experimental Diving Unit; Panama City, FL 323407-5001**

17 COSATI CODES			18. SUBJECT TERMS (Continue on reverse if necessary and identify by block number)
FIELD	GROUP	SUB-GROUP	**elastance, inertance, breathing bag design, impedance testing**

19. ABSTRACT (Continue on reverse if necessary and identify by block number)

This work deals with various aspects of elastance and inertance as they relate to UBA breathing bag design, including non-linear elastance, impedance testing, and methods of inertance reduction and control. The results of this work show that a) nonlinear elastance may be useful in dual breathing bag design but not in single bag designs, b) elastance should be measured statically or quasi-statically rather than dynamically because of potential nonlinearity invalidating forced oscillation analyses, and c) inertance in water column experiments can be virtually eliminated when water is displaced radially rather than axially during tidal breathing. This results from moving water in a manner which minimizes linear accelerations.

20. DISTRIBUTION/AVAILABILITY OF ABSTRACT ☒ UNCLASSIFIED/UNLIMITED ☐ SAME AS RPT ☐ DTIC USERS	21. ABSTRACT SECURITY CLASSIFICATION Unclassified
22a. NAME OF RESPONSIBLE INDIVIDUAL Regina E. Hunt, Command Editor	22b. TELEPHONE (Include Area Code) (301) 295-0198 — 22c. OFFICE SYMBOL MRL/RSP/NMRI

DD FORM 1473, 84 MAR — 83 APR edition may be used until exhausted. All other editions are obsolete.

SECURITY CLASSIFICATION OF THIS PAGE
UNCLASSIFIED

TABLE OF CONTENTS

LIST OF FIGURES

LIST OF TABLES

LIST OF APPENDICES

ACKNOWLEDGMENTS

This study was supported by a Summer Research Fellowship from the Navy/ASEE (American Society for Engineering Education) Program. The views, opinions and/or findings should not be construed as official or reflecting the views, policy or decision of the Navy Department or the naval service at large, unless so designated by other official documentation.

NOMENCLATURE

A = area, cm^2

A_s = cylindrical surface area (curved surface), cm^2

A_x = cross-sectional area, cm^2

D = diameter of base of cone, or cylinder diameter, cm

E = elastance, elastic load, cmH_2O/liter or $Kpa \cdot l^{-1}$

f = cycle frequency, Hz

f_n = natural or resonant cycle frequency, Hz

h = pressure over atmospheric or ambient, gauge pressure, cmH_2O or $kPa \cdot l^{-1}$

h_i = initial air space height for water column container, cm

H = height of cone or pyramid, base to apex, cm

I = inertance, inertial impedance, $cmH_2O/(liters/sec^2)$

L = length, axial length of cylinder, cm

P = pressure, cmH_2O or KPa

ΔP = pressure difference, cmH_2O

R = flow resistance, resistive impedance, $cmH_2O/(liters/sec)$

S.G. = specific gravity, dimensionless

V = volume, liters

V_{ci} = initial volume of air or gas in water column container, liters

V_h = volume due to water column depression or movement from initial condition, liters

V_T = tidal volume, liters

Z = system impedance, $cmH_2O/(liters/sec)$

Z^* = complex impedance, $cmH_2O/(liters/sec)$

$|Z|$ = magnitude of Z^*, $cmH_2O/(liters/sec)$

z_c = axial length of cone or pyramid cap, apex to frustum plane, cm

Greek Symbols

γ = ratio of specific heats, C_p/C_v, dimensionless

ζ = damping coefficient, dimensionless

μ = viscosity, Poise

ρ = density, g/cm^3

τ = system time constant, sec

ω = radian frequency, radians/sec

INTRODUCTION

Gas flow generated by a diver on an underwater breathing apparatus (UBA) is periodic in nature. In a closed-circuit UBA, such as the Navy's Mk-16, breathing impedance comprises flow resistance, elastance and inertance. These impedances result in greater effort expended to move gas through the UBA. From the standpoint of scientific understanding, flow resistance is rather well understood, but elastance, inertance and their interaction are not. In order to model UBA and gain further fundamental understanding of elastance, inertance and their relationship to UBA breathing impedance, this work was undertaken. In an earlier NMRI Technical Report (1) we studied elastance in some detail. In this work further issues concerning elastance are explored, and inertance is studied from a basic experimental viewpoint to explore ways to control it.

Elastance and inertance have important relationships to breathing bag design, water column experiments and simulation of UBA. Nonlinear elastance may help to reduce the elastic load in breathing bag(s). The implications of nonlinear elastance for impedance testing and elastance measurement are discussed also in this work. This has led to establishing criteria for a breathing machine.

The reduction of inertance by changing the path of water displaced by the breathing bag also is explored in this work, and the implications for natural frequency breathing are discussed.

ELASTANCE

Nonlinear Elastance and Breathing Bag Design

Elastance is the change in pressure in response to a volume change in a system. Elastance is the reciprocal of compliance and has the units $kPa \cdot l^{-1}$, cmH_2O/liter, or the equivalent. The pressure-volume characteristic of a closed system or element within that system can be obtained by measuring the pressure difference when the volume is changed, for example, by a tidal volume introduced to the system.

The pressure-volume curve represents the elastance characteristics of any breathing system. When the elastic characteristics are linear, the pressure-volume curve is a straight line, and elastance is the slope of that line. When elastic characteristics are nonlinear, the pressure-volume relationship is curved, and elastance can be defined in two ways. In the tangent method elastance is the slope of the tangent at a point on the P-V curve, for example $E = (\Delta P/\Delta V)_V$. In the secant method elastance is $E = \Delta P/\Delta V$ along the curve, where one of the P,V points is always fixed at a relative origin (0,0). This method gives $\Delta P/V_T$ which is the change in pressure relative to the tidal volume (V_T). We always use the secant method here, because we are generally dealing with tidal volumes. Regardless of the method used to define elastance, the P-V curve should always be obtained for nonlinear systems.

The elastance of a water column is determined by its geometry (1). In a column with vertical sides elastance is essentially linear and inversely proportional to cross-sectional area. This is true because the volume displaced is equal to the area times the vertical excursion of the air-water interface. Since this vertical excursion is essentially equal to the pressure generated (after appropriate units conversions), the definition of elastance, $\Delta P/V_T$ is equal to $(\rho g)h/h \cdot A$, which reduces to $(\rho g)/A$.

A nonlinear pressure-volume curve can be generated by using a container with sloping sides, where cross-sectional area varies with depth of the air-water interface. Both conical and pyramidal shapes were studied in the earlier NMRI Technical Report (1). These shapes offer the possibility of lowering elastic pressures experienced during breathing by increasing the cross-sectional area during a breath. The equations were developed assuming isothermal conditions. Adiabatic conditions result in complications that make an analytical solution impossible for the cone or pyramid, but the solution for the elastance of a rigid, fixed volume container is presented in Appendix A. The polytropic index may prove useful here, if desired, as in Tomlinson, et al (2).

Figure 1 illustrates the effects of orientation and initial gas volume on the elastance of three conical containers of equal size and geometry. The nonlinear shape of the P-V curve is evident in this figure. Two cones have an initial free-space

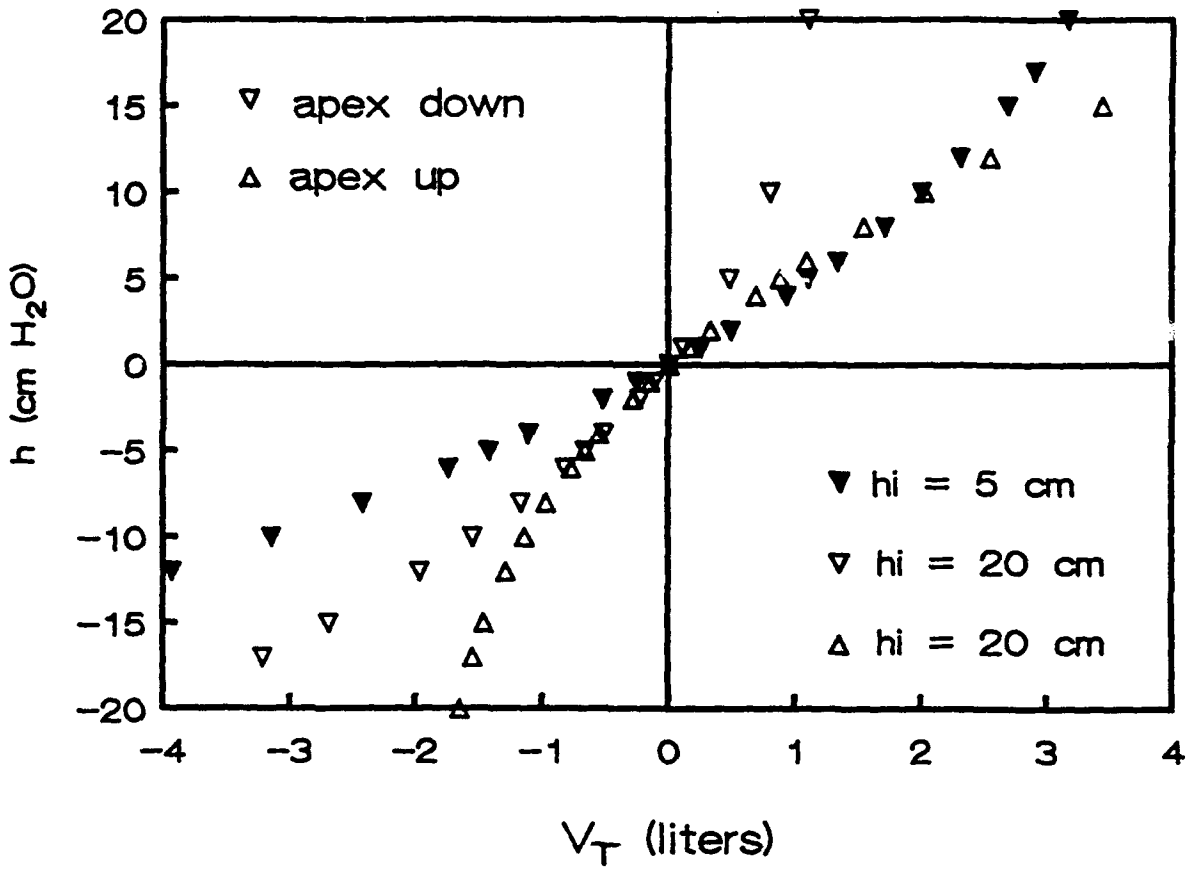

Fig. 1. Pressure-Volume Curves for Conical Bags, Apex Up and Apex Down

volume (V_{ci}) corresponding to an initial free-space height (h_i) of 20 cm, but one is oriented apex up while the other has its apex down. The third cone is oriented apex down and has a 5 cm free-space height. Details of geometry and nomenclature are given in Appendix B. The P-V curves are all asymmetric, because cross-sectional area increases with depth when the orientation is apex up, but decreases when the apex is down. The same volume change spread out over a larger cross-sectional area gives shallower depths, hence smaller pressures and lower elastance. The 20 cm initial free-space height in the apex down position shows highest elastance in the positive pressure region but mid-level elastance in the negative pressure region. The apex up position with h_i = 20 cm shows low elastance in the positive pressure region but high elastance in the negative pressure region, somewhat the opposite. If the apex-down cone has less free-space height, the cone is lower in the water. For an initial height of 5 cm in the apex down position pressures are somewhat lower overall and elastance is lower, because the cross-sectional area is relatively larger than the other two cases.

Using a nonlinear bag in single-bag designs has no advantages, because the reduction in elastance gained on one phase of ventilation would be lost on the other. For example, if the apex up position is used, elastance is reduced on exhalation, but increased on inhalation. The reverse is true for the apex down position. These arrangements, however, may be useful in physiological testing, for example, to determine whether

tolerance for high elastance is on the inhalation or exhalation side, or at the beginning or end of the tidal volume.

Employing a nonlinear elastance to decrease respiratory load in a counterlung can be demonstrated by a dual bag system in which an apex down bag is used for inhalation, and an apex up bag is used for exhalation. Figure 3 shows that such an arrangement, when sized properly, closely approximates the elastance characteristics of the Mk-15 in the vertical position. During inhalation as the air-water interface of the inhalation bag rises, its cross-sectional area increases, thereby reducing elastance. On exhalation, as the air-water interface of the exhalation bag descends, cross-sectional area increases also, again reducing elastance. The practical application of such a dual bag arrangement is complicated by the necessity of interconnecting the bags to provide an unobstructed breathing circuit.

In summary, to minimize elastance in a breathing bag, the cross-sectional area should be as large as practicable. Cubic or spherical shapes may be considered. Dual nonlinear bag designs may be advantageous, but this will depend on the resistance in the communication line and the orientation and size of the bags.

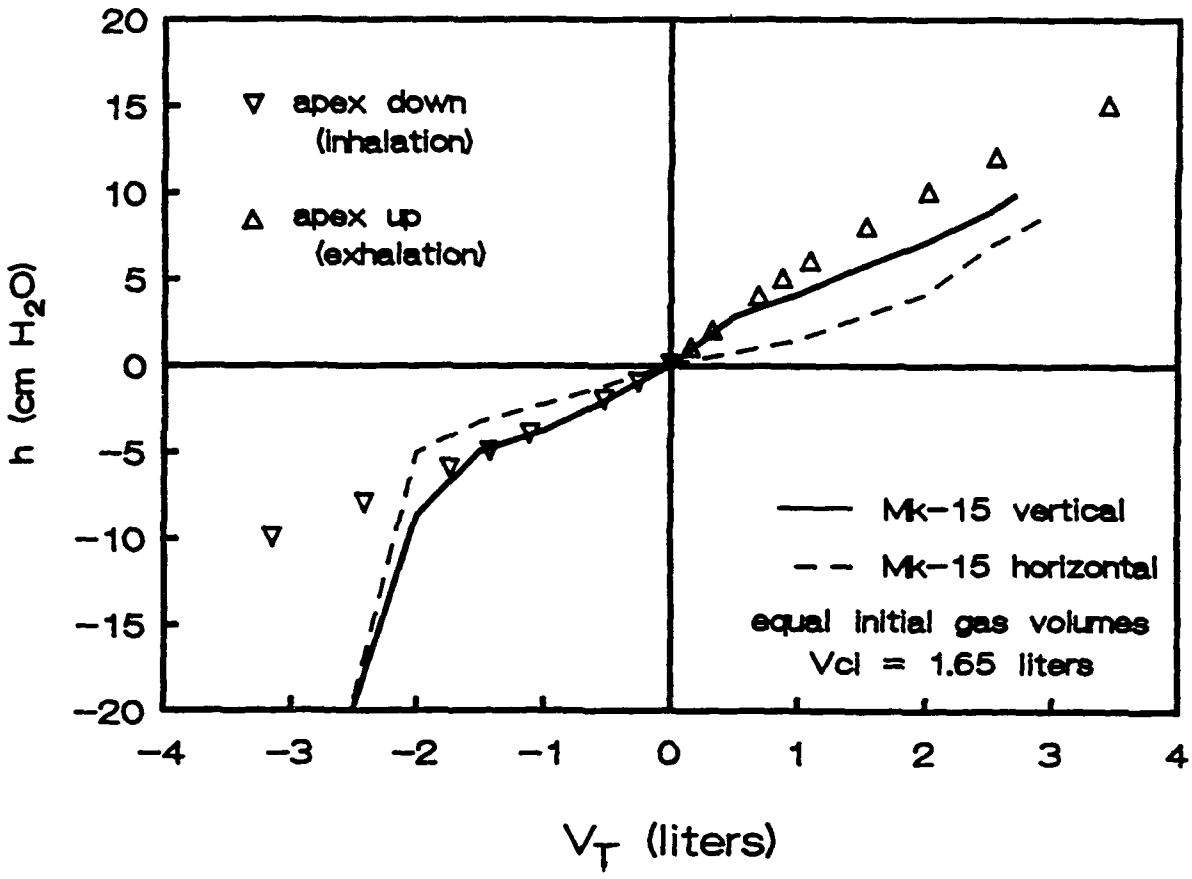

Fig. 2. Pressure-Volume Curves for Mk-15 and Dual Conical Bags

Impedance Testing

Impedance testing with sinusoidal input has been used in physiological studies of respiratory mechanics (3-6). Impedance is the ratio of measured pressure to measured flow and can be represented as a complex number with real and imaginary parts.

$$Z^* = R + (\omega I - E/\omega)j \qquad (1)$$

where Z^* is total (complex) impedance, R is flow resistance, I is inertance, E is elastance and ω is the radian frequency (see Nomenclature for units). The real part of Eqn. (1) is the flow resistance; the imaginary part (the reactance) is the expression in parentheses multiplying "j" and comprises inertance and elastance. When $\omega I = E/\omega$ the reactance is zero, and the impedance is equal to the flow resistance only. This defines the natural or resonant frequency, which is given by $\omega_n = \sqrt{(E/I)}$ in radians/sec. The magnitude of impedance is

$$|Z| = \sqrt{R^2 + (\omega I - E/\omega)^2} \qquad (2)$$

which when multiplied by the flow rate yields the pressure. When peak or average flows are used, the impedance allows peak or average pressures to be calculated (3). Equations for these components of impedance in a variety of different cases, including a water column, are given in Appendix C.

The typical impedance vs. frequency curve for systems with linear components (R, E, I) in series is given in Fig. 3.

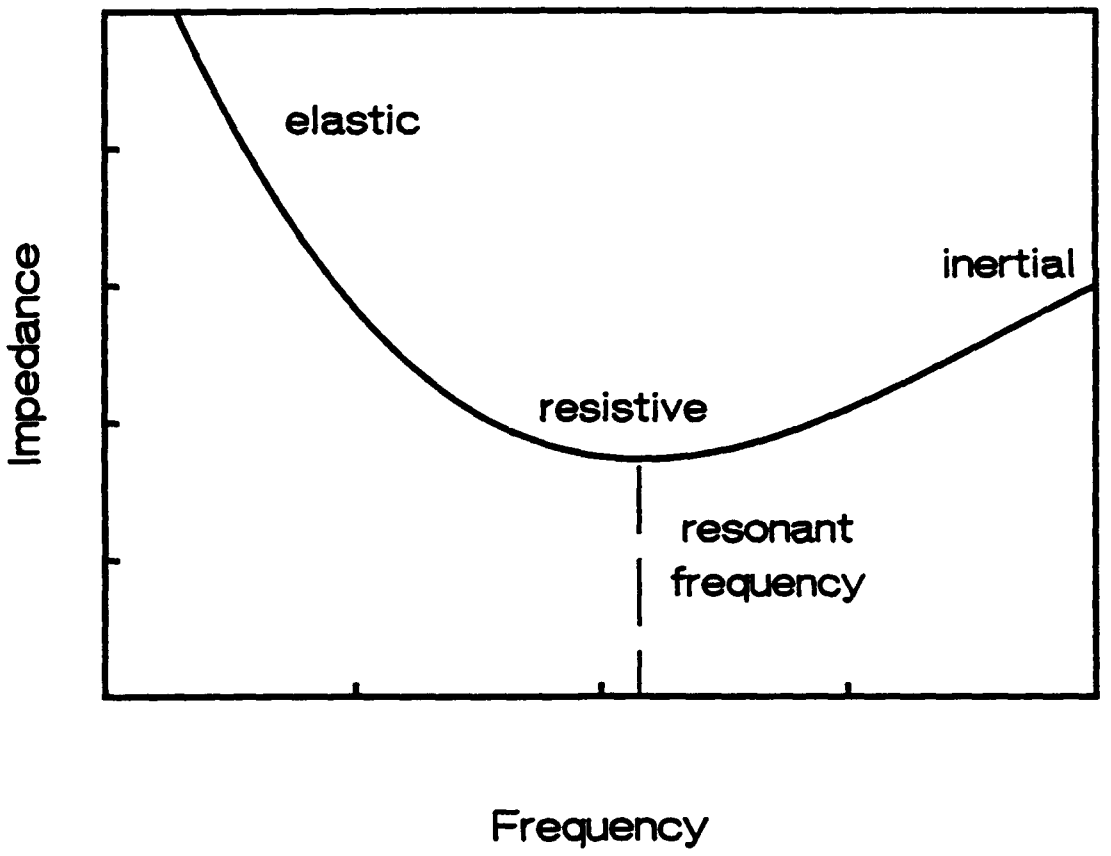

Fig. 3. Impedance Characteristics for System Comprising Linear Elastance, Inertance and Resistance in Series

Impedance at low frequencies is dominated by elastance; at high frequencies inertance is dominant. At the resonant frequency inertial and elastic terms cancel, and impedance equals flow resistance.

The components of impedance describing the human respiratory system have been obtained from experimental data using an acoustical method developed by Jackson and Vinegar (6). In this case a curve similar to that in Fig. 3 is obtained from pressure and flow measurements; their ratio gives the impedance. The components of impedance are extracted by a multi-parameter curve-fit routine using a computer. The technique makes use of a loudspeaker and a controlled frequency sweep in which the tidal volume varies with frequency, having a larger value at low frequencies and a smaller value at high frequencies as a consequence of constant power input. The technique assumes that E, I and R are independent of frequency.

While the use of the acoustic technique has been proposed as a method of quantifying the mechanical characteristics of UBA (7), the technique has limitations. When a UBA is immersed and filled to its operating volume, the airway pressures can exceed the strength of the speaker cone. Balancing the pressures on the other side of the cone is difficult and troublesome. If a larger, rigid cone is substituted, excessive force is required to move the cone.

If elastance is nonlinear, the acoustic technique cannot be used. Nonlinear elastance is a function of tidal volume, which

changes with frequency during the test. Knowing the relationship between V_T and ω will not help, because pressure is the result of other impedances in addition to elastance and thus cannot be used with V_T to calculate elastance. Obtaining a single value from the impedance curve-fit procedure has no meaning. The acoustical technique also uses tidal volumes which are relatively small compared to actual breathing volumes, thus the elastance measured by such a technique will not be accurate if elastance is nonlinear. Even if the tidal volume is large and constant for the low frequency end of the frequency sweep, the elastance calculated by a curve-fit program will only be true for one tidal volume if the elastance is nonlinear. Therefore, the test will have to be repeated many times to determine the elastance or pressure-volume characteristics of the system.

Another difficulty with oscillatory measurement techniques in general is that nonlinear elastance will not be evident from the test. The parameter estimation routine will curve-fit a value for elastance regardless of nonlinearity. It can do this, for example, by using three points on the curve in Fig. 3 and solving Eqn. (1) simultaneously for the three parameters (E, I and R) which are presumed constant. The "elastance" measured by this test may therefore be totally inaccurate.

As an illustrative example, Fig. 4 shows a comparison of three curves in which inertance is very low (natural cycle frequency > 1 Hz, data in Appendix D) and resistance is constant. The lower (solid) curve was generated with linear elastance (5 cm

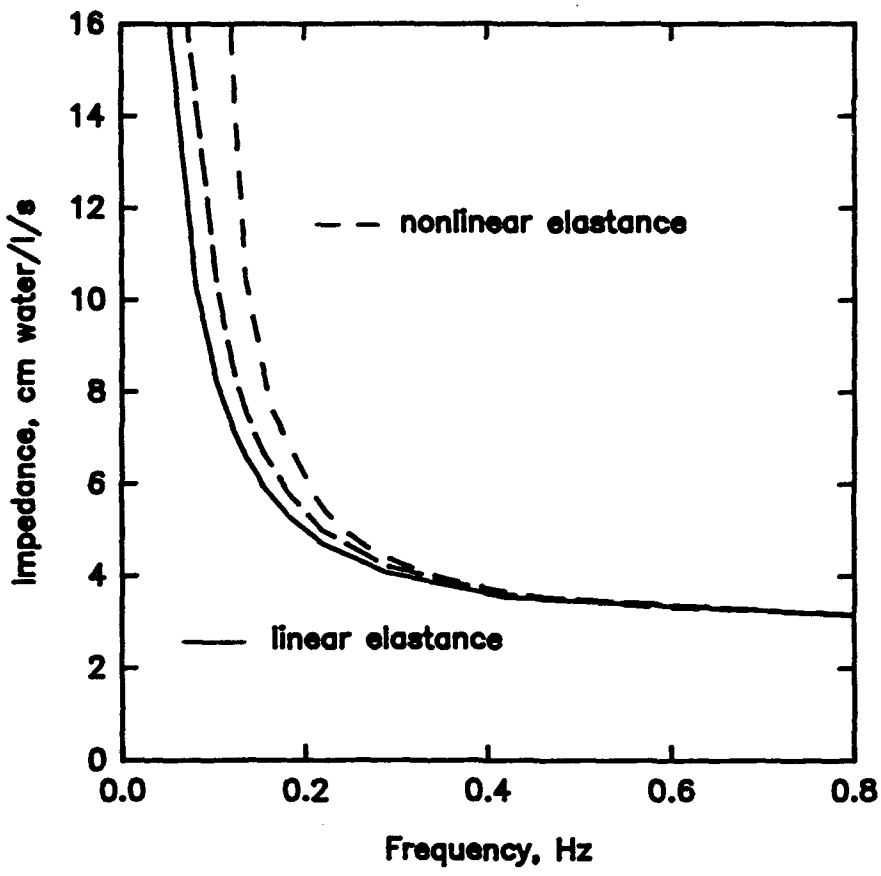

Fig. 4. Impedance Characteristics for Linear and Nonlinear Elastance. Curve with long dashes indicates test run with same $V_T - \omega$ dependence as linear system. Curve with short dashes indicates test run with different dependence

H_2O/liter). The middle (long dashed) curve represents the nonlinear elastance characteristics of a cone (dimensions in Appendix D), apex down and $V_T = 1/\omega$. The elastance varied from 5 to 11.4 cm H_2O/liter at pressures from 1 - 30 cm H_2O, respectively. The upper (short dashed) curve represents a test of the same nonlinear system except that $V_T = 2/\omega$. A single oscillatory test (even with a frequency sweep) will not reveal nonlinearity of elastance. Repeating the test with different tidal volume or tidal volume dependency on frequency will shift the curve as shown. A curve shift or change of impedance at the same frequency is evidence of nonlinear elastance, and a static pressure-volume test should then be performed to determine the elastance characteristics from the P-V curve.

Although the acoustical technique has too many difficulties for application to UBA, oscillatory techniques can still be used. However, any oscillatory technique used for UBA testing should have frequency and tidal volume independently variable and have tidal volumes in the range of actual human breathing. This can be done in a controlled, piston-type breathing machine, such as that built at NMRI for such studies (7). In any oscillatory test, the test should be repeated at least twice at different tidal volumes to check for potential nonlinearity of elastance.

Water Column Experiments

When a water column is used to generate elastance in sinusoidal breathing experiments, the inertance component can be significant (8). Inertance in cylindrical structures for various situations are compared in Table 1. These values were calculated from equations presented in Appendix C. Inertance of the Mk-15 (at 1 ATA in water) is seen to be low, whereas that of an experimental water column apparatus may be twenty times higher! Gas inertance in the tubes at 1 ATA is also low, but can increase

---

TABLE 1

Inertance in Cylindrical Structures, $cmH_2O/(liters/sec^2)$

1. Mk-15 in water at 1 ATA (D = 30 cm, L = 15 cm)	.022
2. Cylindrical Water Column Apparatus (A_x = 56 cm^2, L = 25.4 cm)	.46
3. Air in a Tube at 1 ATA (A_x = 10 cm^2, L = 180 cm, ρ = 1.2 g/liter)	.022
4. Air in a Tube at Depth (appx. 130 fsw) (A_x = 10 cm^2, L = 180 cm, ρ = 6 g/liter)	.11

Values computed by

$\rho L/A = (S.G.)(L)/(.981)(A_x) = cmH_2O/(liters/sec^2)$

---

significantly at depth or with denser gases (4); the increase in inertance is directly proportional to gas density.

Table 2 gives values for resistance, inertance and elastance for another experimental water column apparatus of larger diameter. In this case the resistance of water inside the column is negligible. As a result both inertance and elastance are relatively much more important than resistance. The natural cycle frequency, f_n, for this apparatus (0.74 sec^{-1} or 44 breaths per minute) is within the breathing range. The time constant, τ, is the inverse of the radian natural frequency. Breathing on a water column faster than the natural frequency can generate peak pressures in excess of 60 cm H_2O. Breathing at the natural

---

TABLE 2

Impedances and Time Constant for Water Column Experiments with Sinusoidal Breathing

Water Column Dimensions: D = 10 cm, L = 45 cm, A_x = 78.5 cm^2

Resistance: $R = 8\mu L/A^2$ = .00055 $cmH_2O/(liters/sec)$

Inertance: $I = \rho L/A$ = .585 $cmH_2O/(liters/sec^2)$

Elastance: E = 1000/A = 12.73 $cmH_2O/liter$

Time Constant: $\tau = \sqrt{(I/E)}$ = .2144 sec

Natural Frequency: $f_n = (2\pi\tau)^{-1}$ = 0.74 sec^{-1} ≈ 44 breaths/min

---

A conversion factor, 981/1000, has been applied to the resistance and inertance formulas to convert units to cm H_2O and liters.

frequency minimizes peak-to-peak pressures and improves respiratory comfort.

High inertance may create difficulties when interpreting dynamic water column experiments. In tests with sinusoidal breathing, increases in the inertial load cause high pressures even though the elastic load remains constant. As shown in Table 1, while the elastance of the water column and Mk-15 are equal, inertance in the water column is much higher than that in the Mk-15 under the same conditions. Thus, without inertance reduction the water column does not exactly simulate a diving rig.

Inertance in water column experiments can be reduced in several ways. One method is to shorten the length of the tube. If the tube is too short, however, tidal volume gas will escape. Placing a bag at the end of a shorter tube overcomes this problem and reduces inertance considerably (8). Displacing water radially rather than axially is another method. This decreases inertance by reducing the mass of water moved by a gas displacement of V_T (the amount of water moved is closer to ρV_T rather than $\rho L A_x$), and second, by increasing the area through which the mass of water is displaced (A_s rather than A_x).

Table 3 shows quantitatively the reduction in inertance that was achieved by changing water displacement from axial to radial. This was accomplished in the laboratory test by placing holes in the sides of a container made from perforated steel sheet bent into a conduit with square cross-section 12 cm on a side. A very compliant bag was used to contain the gas. A shorter (hence

lower resistance) flow path for the water exists radially than exists axially (the container is much longer than it is wide).

TABLE 3

Water Column Inertance Reduction by Radial Displacement

Column Dimensions: D= 15 cm, L= 60 cm, A_x= 177 cm^2, A_s = 2827 cm^2

Axial Inertance = $\rho L/A_x$ = mass/A_x^2 = 1(60)/177(.981) =

= .34 $cmH_2O/(liters/sec^2)$

Radial Inertance = mass/A_s^2 = $\rho V_T/(\pi DL)^2$ = 1(2)(10^3)/8(.981)(10^6) =

= .0025 $cmH_2O/(liters/sec^2)$

This permits water to be displaced radially with a minimum of resistance. Using a syringe to generate pressure, the air-water interface moved down, and a strong current of water could be felt by placing a hand near the sides. Almost nothing was felt at the bottom. When the perforations were covered with tape and the experiment repeated, axial currents at the bottom were strong, and radial currents were non-existent.

Figure 5 shows a pressure-time trace of a similar test in which the syringe was given a quick compression stroke and then held. In two tests the holes were open, and in two others the holes were covered with tape. The differences were significant.

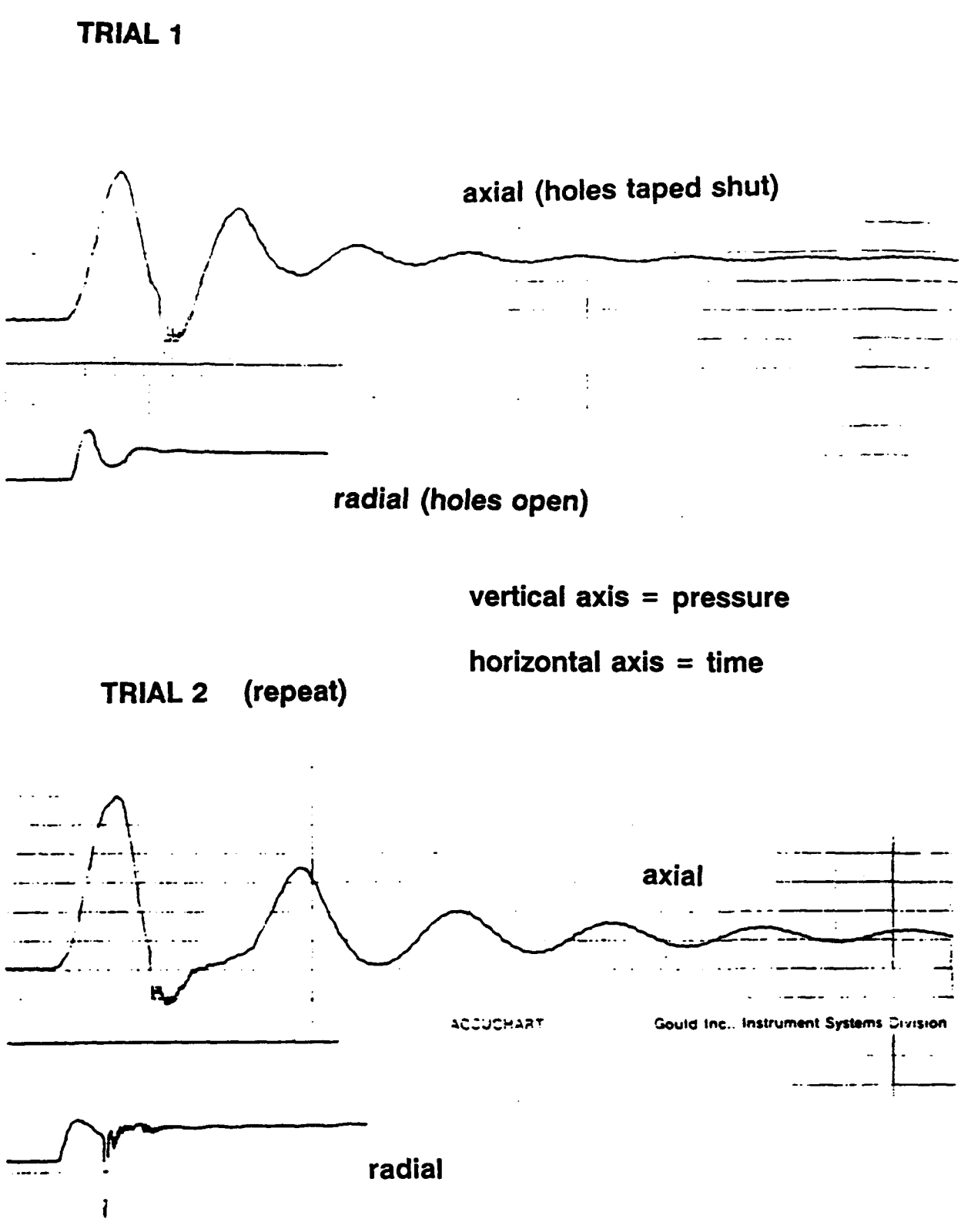

Fig. 5. Cessation of Oscillatory Behavior indicates Inertance Reduction in Water Column Experiments with Perforated-Wall Container (Two Trials)

Lack of overshoot and oscillation show that inertance has been virtually eliminated when the water was allowed to escape through the sides rather than out the bottom.

Breathing Bag Design

Inertance reduction in the water column experiment also has implications for breathing bag design. A design producing unrestricted radial movement (an expanding sphere, for example) would result in minimal inertance. This occurs because linear accelerations are smallest with this geometry. Breathing bags without a surrounding housing, e.g. the EX-19 design, should result in lower inertance than those contained within a housing, such as the Mk-15. In the Mk-15 holes placed around the side of the bag housing rather than at the back, where they now exist, would promote radial displacement of water and reduce inertance without exposing the bag to damage. When water movement caused by the breathing bag is confined by a rigid housing, the housing should be short to minimize axial movement.

Tables 4 and 5 summarize the effects of axial and radial motion using the Mk-15 geometry at pressures of 1 ATA and 130 fsw. In the radial inertance calculation, a 2-liter tidal volume was used. Tidal volume appears in this equation, because the volume of water moved is equivalent to the tidal volume. In the axial case, the volume of water moved is governed by the length of the tube and not the tidal volume (this only fixes the distance moved, not the mass). The elastance of the Mk-15 depends on orientation, but a representative value of 4 cm

H_2O/liter was used (1). A breathing bag design promoting the radial displacement of water gives an inertance more than an order of magnitude lower than a design with axial displacement of water. At depth the inertance of the gas becomes relatively more important and depends on gas density (depth), breathing hose length and diameter. In Table 5, inertance in the Mk-15 from the effects of both the gas (estimated at 1 ATA and at depth) and the water displaced are shown. Total inertance is the sum of both.

TABLE 4

Inertance of the Mk-15 Breathing Bag
with Axial or Radial Path at 1 ATA in Water

Dimensions: D = 30 cm, L = 15 cm, A_x =707 cm^2, A_s = 1413 cm^2

Axial Inertance: $\rho L/A_x = 1(15)/707(.981) =$

$= .0212\ cmH_2O/(liters/sec^2)$

Radial Inertance: $mass/A_s^2 = \rho V_T/A_s^2 =$

$= .0010\ cmH_2O/(liter/sec^2)$

Time Constant: $\tau = \sqrt{(I/E)} = .0728$ sec (axial)

$= .0158$ sec (radial)

Natural Frequency:

$f_n = (2\pi\tau)^{-1} = 2.19\ sec^{-1} = 131$ breaths/min (axial)

$= 10.08\ sec^{-1} = 605$ breaths/min (radial)

The effect of changing to radial inertance at depth has only a small effect on the natural frequency, because inertance due to gas density dominates that due to the movement of water arising from motion of the breathing bag.

TABLE 5

Inertance, Time Constants and Natural Frequencies in the Mk-15 (Simulated) at 1 ATA and at 130 fsw

Inertance, $cmH_2O/(liters/sec^2)$

Water		Gas	
Axial (bag)	Radial (bag)	at 1 ATA	at depth
.021	.001	.022	.110

Time Constant, sec

	axial	radial
1 ATA	.103	.075
130 fsw	.181	.167

Natural Frequency, breaths/min

	axial	radial
1 ATA	93	127
130 fsw	53	57

Natural Frequency Breathing

Ideally, the best UBA design from a respiratory viewpoint is the one that minimizes peak-to-peak mouth pressures for the diver. While the mouth pressure is a function of all three components, the role of inertance is considered to be minor for most practical situations. It is not necessary, however, to eliminate all of the impedance components to obtain the least encumbered breathing. If the UBA could be designed so that its natural frequency coincides with the diver's breathing frequency, flow resistance alone contributes to impedance. By modifying inertance or elastance, the natural frequency of a UBA can be adjusted to the breathing frequency.

Elastance is difficult to adjust, but the possibility exists that inertance "tuning" can be useful as a tool for reducing peak pressures and making breathing more comfortable for the diver. As exercise demands change, the inertance can be altered to "tune" the rig and lower the impediment to breathing. For example, in the Mk-15 inertance can be reduced by opening radial holes instead of axial holes in the breathing bag housing, which reduces the respiratory load at high breathing frequency. Table 5 shows some of the limitations of this. Controlling inertance can also be used to make a UBA breathe the same at 1 ATA and at depth, compensating for the increase inertance of the gas at depth.

The effect of elastance on natural frequency of a UBA is the opposite of that of inertance. A high elastance produces a high

natural frequency, but a high inertance produces a low natural frequency (zero inertance produces infinite natural frequency). High elastance produces increased pressures at frequencies below the natural frequency, whereas high inertance produces increased pressures at frequencies above the natural frequency. If the breathing rate exceeds the natural frequency, higher pressures are generated and breathing becomes uncomfortable.

The interaction of elastance, inertance and resistance should be a fruitful area of study for improved UBA performance and diver comfort and safety. It may also provide a basis for developing assisted-breathing UBA's.

SUMMARY

Nonlinear elastance may have advantages in reducing elastic loads in a dual breathing bag system (apex down for inhalation, apex up for exhalation) by providing increasing cross sectional area on both phases of breathing.

In impedance testing nonlinear elastance poses many problems, and we recommend static pressure-volume data be obtained to determine elastance characteristics of systems with unknown or nonlinear elastance. If impedance tests are used, the tidal volume should be in the breathing range and constant throughout the frequency sweep.

In the water column system inertance can be reduced by shortening tube length and putting a bag around the immersed end

of the tube. Inertance can be virtually eliminated by a design in which water is displaced radially rather than axially, as the air-water interface is moved by gas displacement inside the container.

Varying inertance may be a useful tool for adjusting the natural frequency of a UBA. By matching the UBA natural frequency to the diver's breathing frequency, the respiratory load imposed on a diver can be minimized, thereby improving work capacity and respiratory comfort.

REFERENCES

1. Joye, D.D., Clarke, J.R., Carlson, N.A. and Flynn, E.T., "Formulation of Elastic Loading Parameters for Studies of Closed-Circuit Underwater Breathing Systems", NMRI Technical Report 89-89, Naval Medical Research Institute, Bethesda, Maryland, 1989. available NTIS, Doc. No. ADA-216205.

2. Tomlinson, S.P., Livesey, J., Tilley, D.G. and Himmens, I., "Computer Simulation of Counterlungs", Undersea and Hyperbaric Medicine, 1993: 20(1), pp. 63-73.

3. Peslin, R. and Fredberg, J.J., "Oscillation Mechanics of the Respiratory System", in Fishman, A.P. (ed.), Handbook of Physiology, Section 3: Respiration, Vol. III, Part 2, Chapter 11, American Physiological Society, Bethesda, Maryland; 1986, pp. 145-177.

4. Van Liew, H.D., "The Electrical-Respiratory Analogy when Gas Density is High", Undersea Biomedical Research, 1987: 14(2), pp. 149-160.

5. Clarke, J.R., Survanshi, S. and Flynn, E.T., "Respiratory Waveform Efficiency During Use of Underwater Breathing Apparatus (UBA)", Undersea Biomedical Research, 1990: 17 (Suppl.), p. 31. Abstract #12.

6. Jackson, A.C. and Vinegar, A., "A Technique for Measuring Frequency Response of Pressure, Volume, and Flow Transducers", J. Appl. Physiol.:Respir. Environ. Exercise Physiol., 1979: 47(2), pp. 462-467.

7. Clarke, J.R., Carlson, N.A., Mints, W.H. and Thalmann, E.D., "New Procedures for the Testing of Underwater Breathing Apparatus", Undersea Biomedical Research, 1992: 19 (Suppl.), p. 102, Abstract #170.

8. Carlson, N.A., Clarke, J.R. and Flynn, E.T., "A Technique for independently Varying Inertance and Elastance in Studies of Underwater Breathing Apparatus (UBA), Undersea Biomedical Research, 1990: 17 (Suppl.), p. 152, Abstract #255.

APPENDIX A: DERIVATION OF ELASTANCE FOR A RIGID CONTAINER UNDER ADIABATIC CONDITIONS

For adiabatic conditions the ideal gas law can be written,

$$P_i \cdot V_i^{\gamma} = P_f \cdot V_f^{\gamma} = \text{constant}$$

The general equation for rigid container plus tubing and syringe volumes is,

$$\frac{P_f}{P_i} = \frac{(V_{si} + V_x + V_{con})^{\gamma}}{(V_{si} + V_x \quad V_{con} - V_T)^{\gamma}}$$

or

$$1 + h/P_i = V_{sumi}^{\gamma}/(V_{sumi} - V_T)^{\gamma}$$

and

$$h = P_i \cdot \frac{V_{sumi}^{\gamma} - (V_{sumi} - V_T)^{\gamma}}{(V_{sumi} - V_T)^{\gamma}}$$

Taking the derivative with respect to V_T,

$$dh/dV_T = E = P_i \cdot \frac{d}{dV_T}\left[\frac{V_{sumi}^{\gamma}}{(V_{sumi} - V_T)^{\gamma}} - 1\right]$$

$$= P_i \cdot V_{sumi}^{\gamma}(-\gamma(V_{sumi} - V_T)^{-\gamma-1}(-1)$$

$$= \gamma P_i V_{sumi}^{\gamma}/(V_{sumi} - V_T)^{\gamma+1}$$

for $V_{sumi} \gg V_T$,

$$dh/dV_T = \gamma P_i/V_{sumi} = \gamma\ P_0/V_0.$$

APPENDIX B: CONE DIMENSIONS AND DATA FOR FIGURES 1 AND 2.

The equations for a conical shape are:

Cone, Apex Up

$$V_T = (\pi D^2/12H^2)(h/1000)[h^2 + 3h(h_i + z_c) + 3(h_i + z_c)^2] \quad (1)$$

Cone, Apex Down

$$V_T = (\pi D^2/12H^2)(h/1000)[h^2 - 3h(H - h_i) + 3(H - h_i)^2] \quad (2)$$

where V_T is tidal volume, H is height dimension of the cone from base to apex, h is the depth (+) or height (-) of water in the container relative to that outside the container (h is also gauge pressure), h_i is the initial height of gas space in the container, z_c is the height of the top (apex) part of the cone removed to create a frustum, and D is the cone base diameter. These dimensions are illustrated in Fig. 6 for both cases. Equations 1 and 2 are dimensional with V_T in liters and all distances in cm.

Cone Dimensions: D = 20 cm, H = 50 cm, z_c = 15 cm

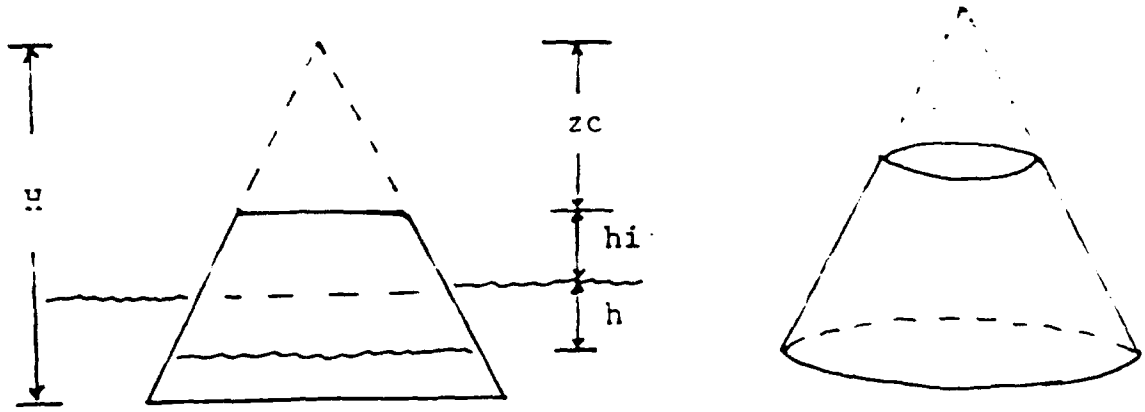

APEX UP

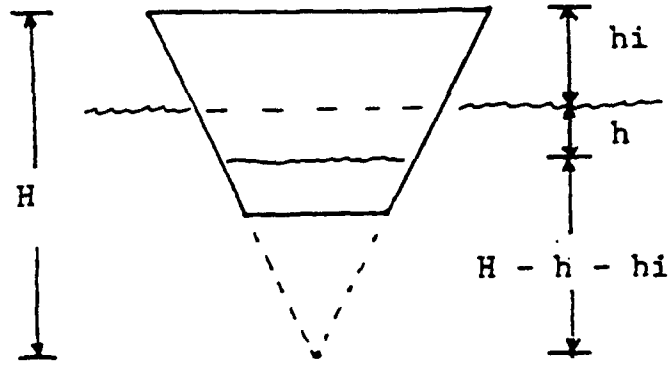

APEX DOWN

Fig. 6. Cone Dimensions and Orientations

APPENDIX B (cont.)

A. Figure 1

1. h_i = 5 cm, cone apex down

V_T, liters	h, cm H_2O
0	0
.25	1
.49	2
.93	4
1.10	5
1.33	6
1.70	8
2.0	10
2.31	12
2.69	15
2.90	17
3.16	20
-.26	-1
-.53	-2
-1.11	-4
-1.42	-5
-1.74	-6
-2.42	-8
-3.15	-10
-3.94	-12

2. h_i = 20 cm, cone apex down

V_T, liters	h, cm H_2O
0	0
.11	1
.48	5
.80	10
1.1	20
-.12	-1
-.24	-2
-.52	-4
-.66	-5
-.82	-6
-1.17	-8
-1.55	-10
-1.97	-12
-2.69	-15
-3.22	-17

3. h_i = 20 cm, cone apex up

V_T, liters	h, cm H_2O
0	0
.16	1
.33	2
.69	4
.88	5
1.09	6
1.53	8
2.02	10
2.55	12
3.44	15
-.15	-1
-.29	-2
-.55	-4
-.66	-5
-.77	-6
-.97	-8
-1.14	-10
-1.29	-12
-1.46	-15
-1.55	-17
-1.65	-20

B. Figure 2

Data for Mk-15 from reference (1)

Data for composite curve: negative pressures from Fig. 1, h_i = 5 cm, cone apex down; positive pressures from Fig. 1, h_i = 20 cm, cone apex up

APPENDIX C: SUMMARY OF EQUATIONS FOR IMPEDANCE COMPONENTS

Peslin and Fredberg (3) summarize basic impedance relationships for sinusoidal inputs. The impedance (Z) is a complex quantity with the real part being the resistance and the imaginary part combining inertance and elastance according to Eqn. 3. In the following, τ is the system time constant, f_n is the natural or resonant frequency, and ζ is the damping coefficient. If the damping coefficient is 1.0, the system is said to be critically damped (no oscillations occur in response to a system disturbance). If the damping coefficient is less than 1, the system is underdamped, and oscillatory behavior is expected. If the damping coefficient is greater than 1, the system is overdamped, and a smooth time response rather than oscillatory behavior is expected.

Resistance: $R = f(\text{geometry, flow, } \omega, \rho, \mu)$

Elastance: $E = \gamma P_0/V_0$ (adiabatic, rigid container)

$= P_i/V_i$ (isothermal, rigid container)

Inertance: $I = n\rho L/A$ (n=1 for flat velocity profile, n=4/3 for parabolic profile)

$I = \text{mass}/A^2$

Time Constant: $\tau = \sqrt{(I/E)}$

Natural Frequency: $f_n = (2\pi\tau)^{-1}$

Damping Coefficient: $2\zeta\tau = R/E$, Thus $\zeta = R/2\sqrt{(IE)}$

For a Cylindrical Water Column with Nonporous Sides:

$R = 8\mu L/A^2$ (for laminar flow, linear resistance)

$E = 1/A$

$I = \rho L/A = \text{mass}/A^2$

Units conversion factors must additionally be used to obtain the units of cm H_2O and liters.

In water column experiments, resistance and inertance cannot be defined exactly. Both are a function of mass which is not constant, since the level of water inside the cylinder changes with pressure.

APPENDIX D: IMPEDANCE TEST SIMULATION AND DATA FOR FIGURE 4.

1. Data for Figure 4: Linear and Nonlinear Elastance in Impedance Tests

f_{12}, Hz	ω, rad/s	Z_1	Z_2	V_T	E_2	h	f_{3}, Hz	Z_3
.7962	5.00	3.16	3.16	.20	5.0	1	.8376	3.16
.4188	2.63	3.55	3.61	.38	5.3	2	.5732	3.35
.2866	1.80	4.09	4.24	.56	5.4	3	.4363	3.61
.2182	1.3	4.72	5.01	.73	5.5	4	.3631	3.91
.1815	1.14	5.31	5.83	.88	5.7	5	.3089	4.24
.1545	0.97	5.96	6.69	1.03	5.8	6	.2707	4.59
.1353	0.85	6.60	7.56	1.18	5.9	7	.2420	5.01
.1210	0.76	7.23	8.57	1.31	6.1	8	.2229	5.41
.1115	0.70	7.75	9.49	1.43	6.3	9	.2086	5.83
.1035	0.65	8.26	10.44	1.55	6.5	10	.1624	7.65
.0812	0.51	10.25	14.39	1.95	7.2	14	.1354	10.46
.0478	0.42	16.90	20.50	2.35	8.5	20	.1210	15.30
							.1168	25.00

Cone with h_i = 10 cm, D = 20 cm, H = 50 cm, z_c = 15 cm

$V_T = 4.19 \times 10^{-5} (h^3 - 120\ h^2 + 4800\ h)$

R = 3

$Z = \sqrt{(9 + E^2/\omega^2)}$

Z_1 is linear, Z_2 and Z_3 are nonlinear (same model, different frequency-tidal volume dependence).